Kodaikanal Obs. Bull. Ser. A (1979) 2, 203-212

R_{II} PARTIAL FREQUENCY REDISTRIBUTION FUNCTION AND ITS EFFECTS ON THE FORMATION OF LINES IN EXPANDING SPHERICAL ATMOSPHERES

A. PERAIAH

ABSTRACT

The redistribution in frequency in lines formed in atmospheres in which the matter is moving radially outwards with velocity gradients is studied in the rest frame of the star. We have considered the R_{II} angle averaged function (See Hummer 1962) with radiation damping in the atom's rest frame and assumed a non-LTE two level atom.

We have considered B/A = 1, 10 and 100 where B/A is the ratio of outer to inner radii of the medium. The maximum velocities at the outer most layers are taken to be 1 and 2 units of mean thermal velocity. Two cases of line emission and line and continuum emission are calculated. In either case we have taken the optical thickness of the medium to be approximately 10^3. For comparison lines formed with complete redistribution (CRD) have been presented for all cases of velocity distribution and geometrical thickness.

A very striking fact emerges from these calculations. The emission or absorption is correspondingly larger or deeper in the case of lines formed in CRD than those formed with the R_{II} angle averaged function. In static spherically symmetric medium the emergent mean intensities Jx show up in emission where as those in plane parallel case show up in absorption when there is emission from continuum and profiles in spherical symmetry show emission in the wings. In the differentially moving medium, we notice red emission and blue absorption while the centre of the line is shifted towards violet side. P cygni type profiles are noticed in the presence of continuum and line emission.

Key words: RII partial frequency redistribution function—radiative transfer in spherical symmetry—expanding atmospheres

1. Introduction

During the processes of absorption and emission of a photon by an atom, redistribution of photon occurs due to scattering. This redistribution of photons could be either complete or partial over the line. Complete redistribution need not be accomplished in stellar atmospheres and strictly speaking one has to consider the redistribution not only in frequency but also in angle. This becomes more important when one considers spherical atmospheres with translatory gaseous motions, either radial or non-radial. The major change introduced by the redistribution function occurs through the scattering integral given by

$$\frac{1}{\phi(x,\mu)} \int_{-1}^{+1} \int_{-\infty}^{+\infty} R(x,\mu;x',\mu')\, I(x',\mu')\, dx'\, d\mu'$$

where $x = (\nu - \nu_0)/\Delta\nu$, ν_0 being the central frequency and $\Delta\nu$ is some standard frequency interval, and $\phi(x,\mu)$ is the profile function given by

$$\phi(x,\mu) = \int_{-1}^{+1} \int_{-\infty}^{+\infty} R(x,\mu,x',\mu')\, dx'\, d\mu'$$

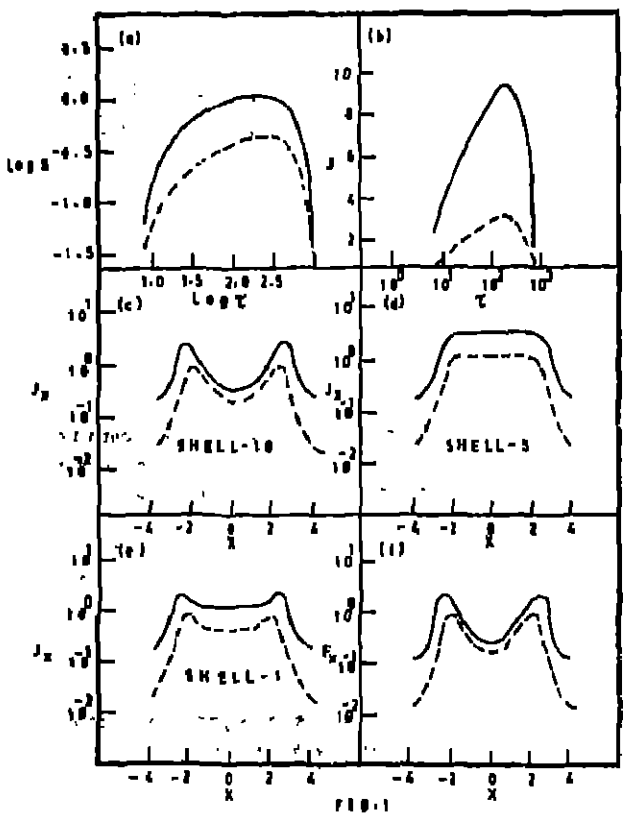

FIG.1

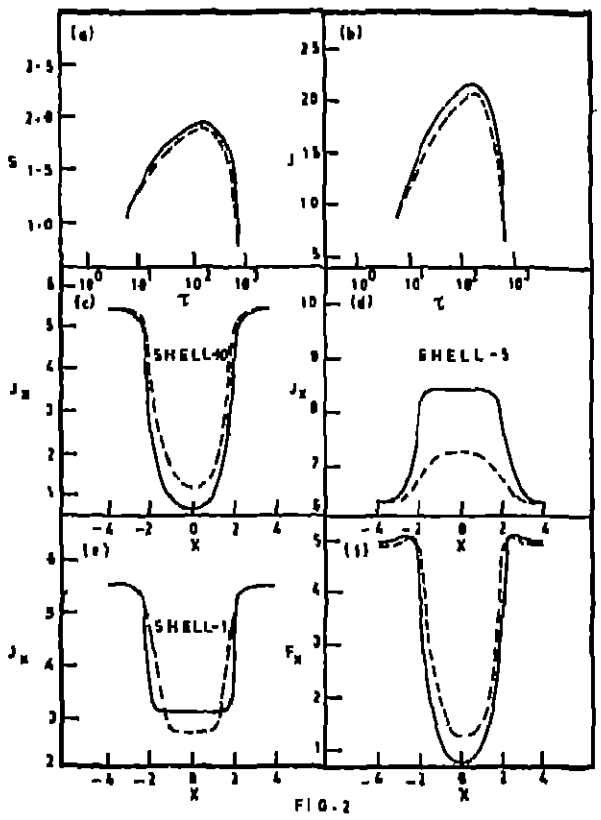

FIG.2

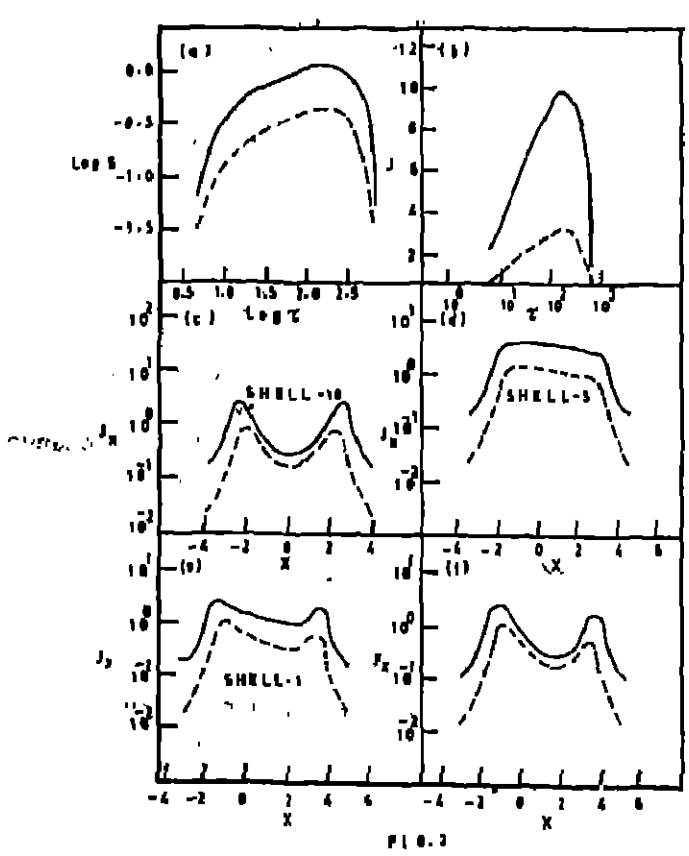

FIG.3

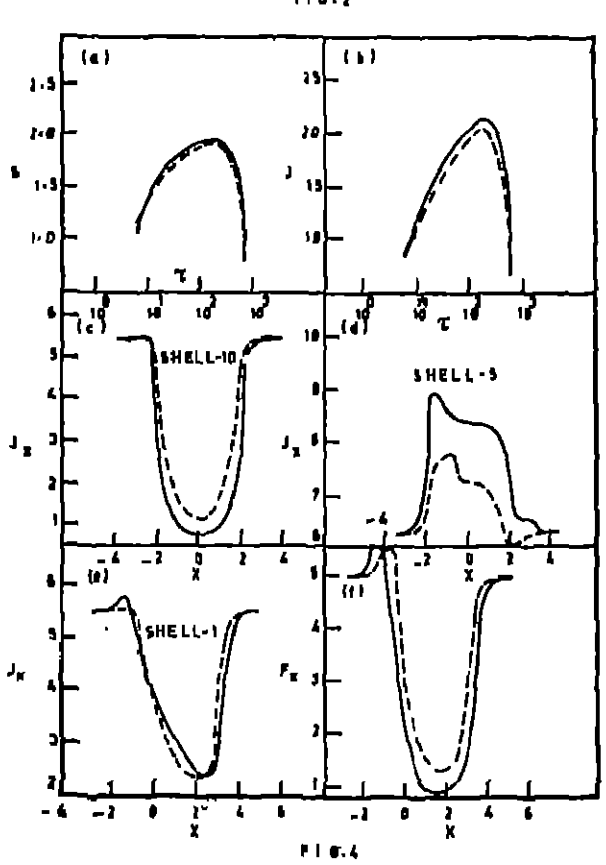

FIG.4

Fig. 1 & 2 V=0 B/A=1 Fig. 3 & 4 V=1 B/A=1. Fig. 1 & 3 $\epsilon=10^{-3}$ $\beta=0$. Fig. 2 & 4 $\epsilon=\beta=10^{-3}$. ____ CRD, ---- RII - is common for all figures.

and R (x, μ, x', μ') is the redistribution function, I (x', μ') is the specific intensity of the scattered beam making an angle $\cos^{-1}\mu'$ with the radius vector with redistributed frequency x' with initial frequency x incident at angle $\cos^{-1}\mu$ with the radius vector. In the case of complete redistribution of frequencies over the whole line, the scattering integral reduces to

$$\int_{-\infty}^{+\infty} \phi\ (x,\ \mu)\ I\ (x,\ \mu')\ d\mu'\ dx$$

As one can see from the two scattering integrals of (one with redistribution and the other with the profile function), a detailed account of the photon redistribution is possible only when one considers the R introduction of the R (x, μ ; x', μ') function in the scattering integral. In a moving medium the redistribution function becomes strongly dependant on angle and the frequencies of incidence and scattering x and x' become $x \pm \mu v$ and $x' \pm \mu v$ for the oppositely directed beams of radiation where v is the radial velocity of the gas in mean thermal units. This angle dependance of the frequency occurs irrespective of the fact whether or not we consider angle averaged redistribution function. It is necessary that one must take into account of the angle dependance simply because of the fact that in spherically symmetric approximation the angle made by the ray with the radius vector continually changes with radius and the frequency is modified by this process known as curvature scattering (see Peraiah and Grant 1973). However, the inclusion of angle in these calculations increase the amount of effort on computer considerably. A thorough study of the angle dependance has been implemented on R_I function for both isotropic and dipole scattering media (Peraiah 1978 b). This study has shown that there are observationally noticeable differences between the lines formed by using angle dependant and angle independant redistribution functions. Several authors have studied the effects of these functions on the formation of spectral lines in stellar atmospheres in plane parallel approximation (Hummer 1962, 1969, Shine *et al.* 1975, Vardavas 1976, Mihalas 1978).

The effects of partial frequency redistribution in expanding spherical atmospheres has been studied to some extent in detail by Peraiah (1978b ; 1979), Peraiah and Wehrse (1978). In the above studies, we have confined mostly to the effects of R_I function for zero natural line width. However, it is of great interest to study the effects of R_{II} partial redistribution function as it represents scattering by a resonance line broadened by radiation damping. This function has been studied by Jefferies and White (1960).

As a first step, in this paper the effects of angle averaged redistribution function R_{II} on the formation of lines in expanding spherical media are investigated.

2. A Brief Description of the Method

The method has been described in detail in Peraiah (1978b). We shall employ the angle averaged redistribution function R_{II} given by,

$$R_{II}(x, x') = \frac{1}{\pi^{3/2}} \int_{\frac{1}{2}|\mathfrak{X}-\mathfrak{x}|}^{\infty} e^{-u^2} \left\{ \tan^{-1}\left(\frac{\mathfrak{X}+u}{a}\right) - \tan^{-1}\left(\frac{\mathfrak{x}-u}{a}\right) \right\} du \qquad (1)$$

where $\mathfrak{X}$ and $\mathfrak{x}$ are correspondingly the maximum and minimum values of x and x' and x ($= (\nu - \nu_0)/\Delta s$) and x' ($= (\nu' - \nu_0)/\Delta s'$, Δs being some convenient frequency interval) are the frequencies of the absorbed and emitted photon. The equation of radiative transfer in spherically symmetric media for a non-L.T.E two-level atom model is written as

$$\mu \frac{\partial I\ (x,\ \mu,\ r)}{\partial r} + \frac{1-\mu^2}{r} \frac{\partial I\ (x,\ \mu,\ r)}{\partial \mu} = K_L\ [\beta + \phi\ (x,\ \mu, r)]\ [S(x,\ \mu,\ r) - I\ (x,\ \mu, r)] \qquad (2)$$

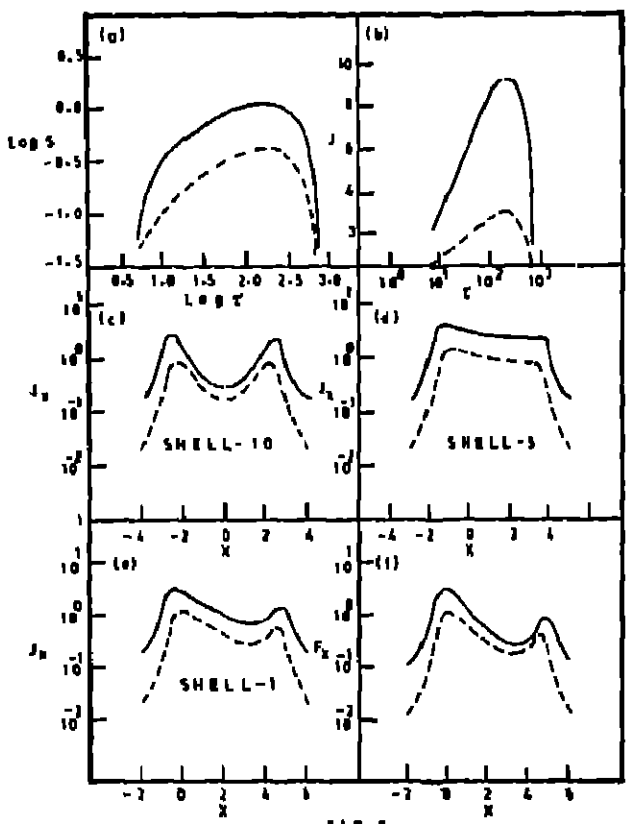

FIG. 5

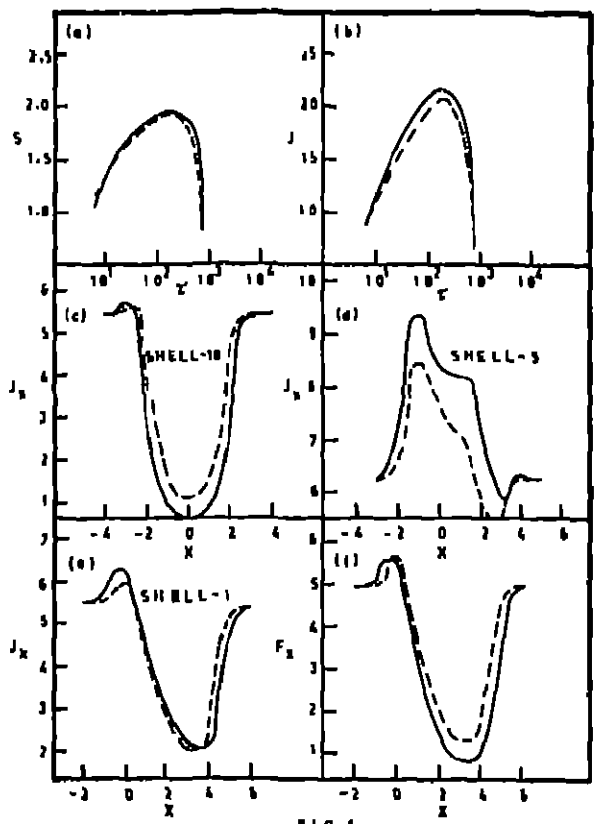

FIG 6

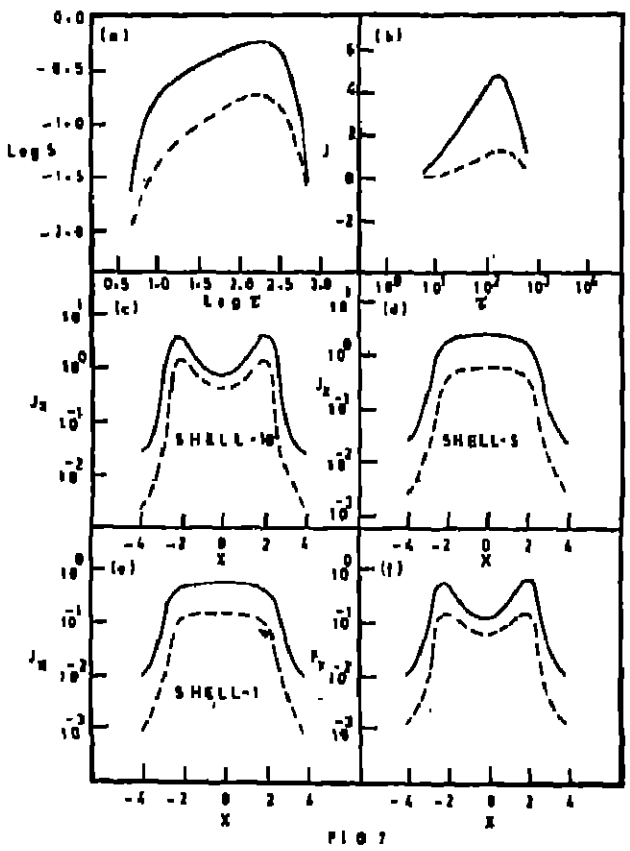

FIG 7

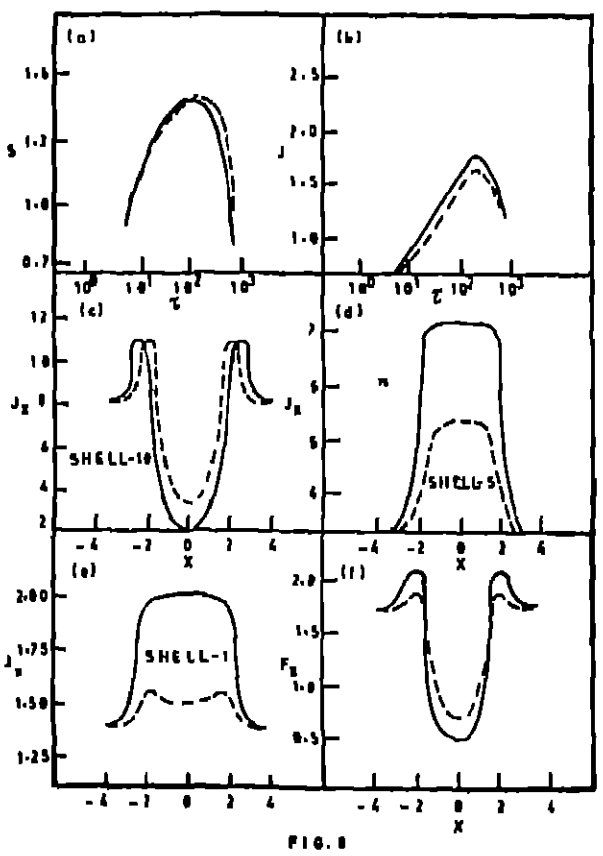

FIG. 8

Fig. 5 & 6 V=2 B/A=1. Fig. 7 & 8 V=0 B/A=10. Fig. 5 & 7 $\epsilon = 10^{-3}$ $\beta=0$ Fig. 6 & 8 $\epsilon = \beta = 10^{-3}$. _CRD ---- RII - ip common for four figures.

and for oppositely directed beam,

$$-\mu \frac{\partial I(x, -\mu, r)}{\delta r} - \frac{1-\mu^2}{r} \frac{\partial I(x, -\mu, r)}{\delta \mu} = K_L [\beta + \phi(x, -\mu, r)] [S(x, -\mu, r) - I(x, -\mu, r)] \quad (3)$$

Here $I(x, \mu, r)$ is the specific intensity of the ray making an angle $\cos^{-1}\mu$ ($\mu \in [0, 1]$) with the radius vector at the radial point r with frequency $x (= (\nu - \nu_0)/\Delta\nu$, $\Delta\nu$ being some convenient frequency interval). The source function $S(x, \pm\mu, r)$ is given by,

$$S(x, \pm\mu, r) = \frac{\phi(x, \pm\mu, r) S_L(x, \pm\mu, r) + \beta S_c(r)}{\phi(x, \pm\mu, r) + \beta} \quad (4)$$

Where β is the ratio of K_c/K_L of opacity due to continuous absorption per unit interval of x to that in line centre and $\phi(x, \pm\mu, r)$ is the profile function, $S_L(x, \pm\mu, r)$ and $S_c(r)$ are the source functions in line and continuum and are given by,

$$S_c(r) = \rho(r) B(\nu_0, T_e(r)) \quad (5)$$

where $\rho(r)$ is an arbitrary factor and $B(\nu_0, T_e(r))$ is the Planck function for frequency ν_0 at temperature Te and

$$S_L(x, \pm\mu, r) = \frac{(1-\epsilon)}{\phi(x, \pm\mu, r)} \int_{-\infty}^{+\infty} dx' \int_{-1}^{+1} R_{II}(x, \pm\mu; x', \mu') I(x', \mu') d\mu' + \epsilon B(r) \quad (6)$$

and

$$\epsilon = \frac{C_{21}}{C_{21} + A_{21}[1 - \exp(-h\nu_0/_{kT})]^{-1}} \quad (7)$$

is the probability per scatter that a photon is destroyed by collisional de-excitation. We have treated two cases : (1) $\epsilon = 10^{-3}$, $\beta = 0$ and (2) $\epsilon = \beta = 10^{-3}$. We have to solve the two equations (2) and (3) by specifying the quantities ϵ, β, ρ (<1), R_{II} and B in advance and we have set the line centre optical depth to be equal to 10^3, Evaluation of the redistribution function R_{II} appearing in the scattering integral should be done accurately. For a static medium, we need to calculate R_{II} function only once as this is angle averaged where as when the gases are in motion the frequencies change because of Doppler shifts and we have to evaluate four functions :

$$R_{II}(x+\mu v ; x'+\mu v), \quad R_{II}(x-\mu v ; x'+\mu v),$$

$$R_{II}(x-\mu v ; x'-\mu v) \text{ and } R_{II}(x+\mu v ; x'-\mu v).$$

As we can see there is no symmetry among these functions and all the functions must be calculated at each radial point. The normalizing condition for the redistribution function is (See Peraiah 1978a)

$$\frac{1}{4} \sum_{l=1}^{K} \sum_{m=1}^{K} [R_{II,}{}^{++}{}_{lm} W_l^{++} W_m^{++} + R_{II,}{}^{-+}{}_{lm} W_l^{-+} W_m^{-+}] = 1 \quad (8)$$

where

$$W_{l,\,m} = a_l c_j, \quad a_l = \frac{A_l R_{II,\,lm}}{\sum_{l,\,m=1}^{K} R_{II,\,lm} A_l C_j}$$

where A's and C's are the quadrature weights for frequency and angle points respectively.

and $[k, l, m] \equiv [J + (l-1) J]$

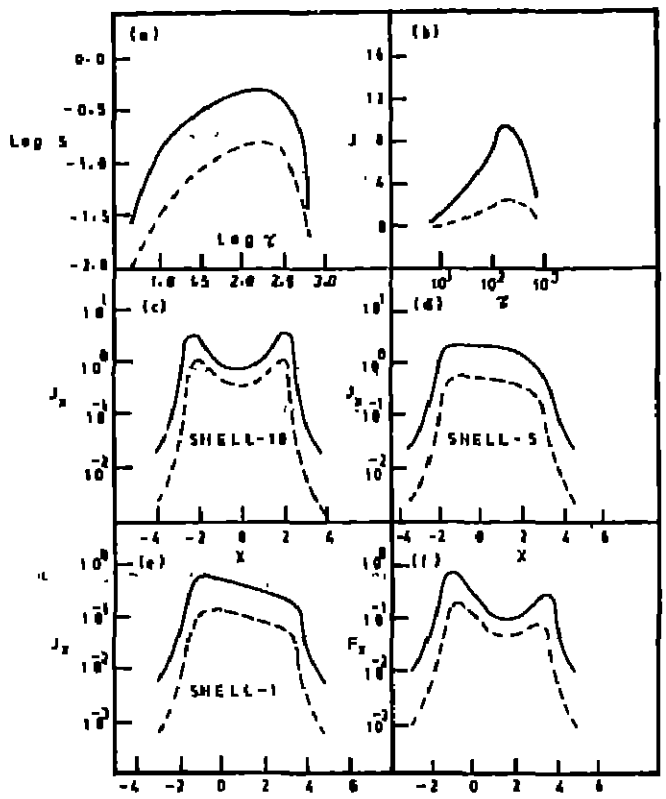

FIG 9

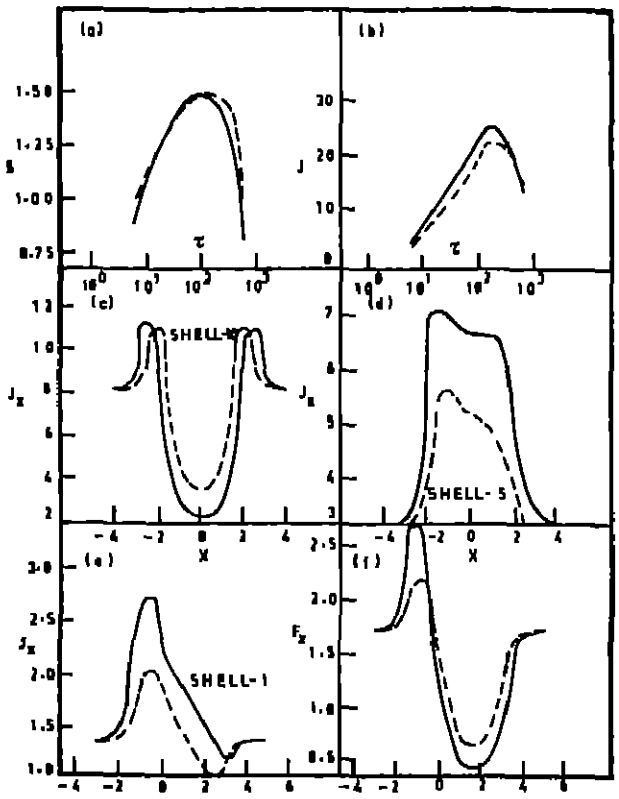

FIG 10

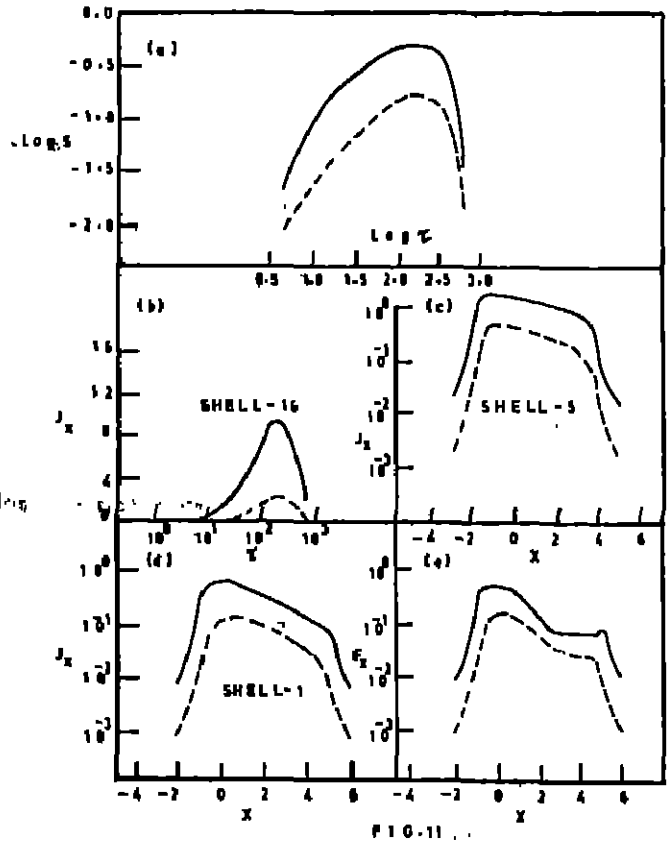

FIG-11

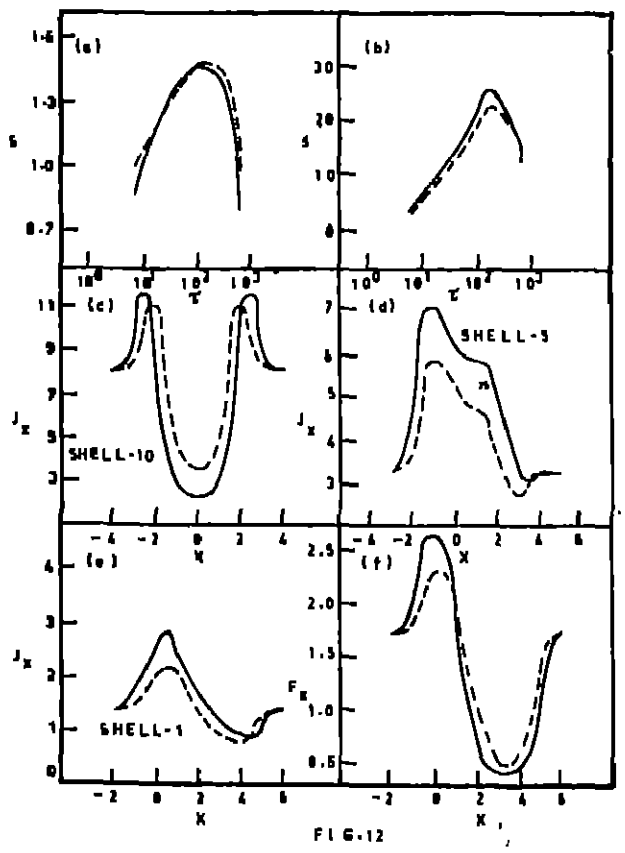

FIG-12

Fig. 9 & 10 V=1 B/A=10 Fig. 11 & 12 V=2 B/A=10, Fig. 9 & 11 $\epsilon = 10^{-3}$ $\beta = 0$. Fig. 10 & 12 $\epsilon = \beta = 10^{-3}$. ____ CRD ---- RII - is common for all figures.

i, J being the running indices for frequency and angle point and J is the total number of angle points.

The symbols R_{II}^{++} and R_{II}^{-+} represent,

$$R_{II}^{++} = R_{II}(x+\mu v\,;\ x'+\mu v)$$

and

$$R_{II}^{-+} = R_{II}(x-\mu v\,;\ x'+\mu v)$$

where v is the radial velocity of the gas in units of mean thermal velocity of the gas. Similarly R_{II}^{+-} and R_{II}^{--} are defined. The profile function of the line for partial frequency redistribution is calculated from the relation

$$\phi_x^{+} = \phi_x(+\mu) = \tfrac{1}{2}\sum_{l=1}^{I}\sum_{j=1}^{m}[R_{kl}^{++}{}_{lj} + R_{kl}^{-+}{}_{lj}]\,a_l\,c_j \tag{10}$$

Calculations of the diffuse reflection, transmission functions have been performed as described in Peraiah (1978b). In the next section we shall discuss the results.

3. Results and Discussion

We have computed line profiles in plane parallel and spherically symmetric geometries to find out the geometrical effects. The quantity B/A, ratio of outer to inner ratio is set equal to 1 for plane parallel geometry and 10, 100 for spherically symmetric geometry.

The profiles formed with partial redistribution (PRD) are compared with those formed with complete redistribution (CRD) by using Voigt profile function. We have used the algorithm due to Beschek *et al* (1966) to calculate Voigt function assuming a damping constant equal to 10^{-3}. No incident radiation on either side of the medium is assumed, that is

$$U_l^{+}(x_l, \tau=0; \mu_j) = U_{N+1}^{-}(x_l, \tau=T, \mu_j) = 0 \tag{11}$$

where $U_l^{+}(x_l, \tau=0, \mu_j) = 4\pi R_{out}^2 I(x_l, R_{out}, \mu_j)$

and $U_{N+1}^{-}(x_l, \tau=T, \mu_j) = 4\pi R_{in}^2 I(x_l, R_{in}, \mu_j)$

R_{out} and R_{in} are outermost and innermost radii of the medium. N is the total number of shells into which the medium has been divided. For reasons see equation (19) of Peraiah (1978a). The quantity B (r) is set equal to

$$B(\bar{r}) = \frac{1}{4\pi\,\bar{r}^2} \tag{12}$$

where $\bar{r}$ is the mean radius of the shell. The frequency and angle independant source function is calculated by the expression in discrete form

$$S(\tau_n) = \sum_{l=1}^{I}\sum_{j=1}^{J} S(x_l, \mu_j\,;\ \tau_n)\,A_l\,C_j \tag{13}$$

and the monochromatic flux is calculated by

$$F(x_l) = \left(\frac{A}{B}\right)^2 \sum_{j=1}^{J} U_l^{-}(x_l, \mu_j\,;\ \tau=0)\,C_j\,\mu_j \tag{14}$$

The frequency dependant mean intensities are calculated by the expression

$$J_n(x_l) = \tfrac{1}{2}\sum_{j=1}^{J} C_j\,[U_n^{+}(x_l, \mu_j) + U_n^{-}(x_l, \mu_j)] \tag{15}$$

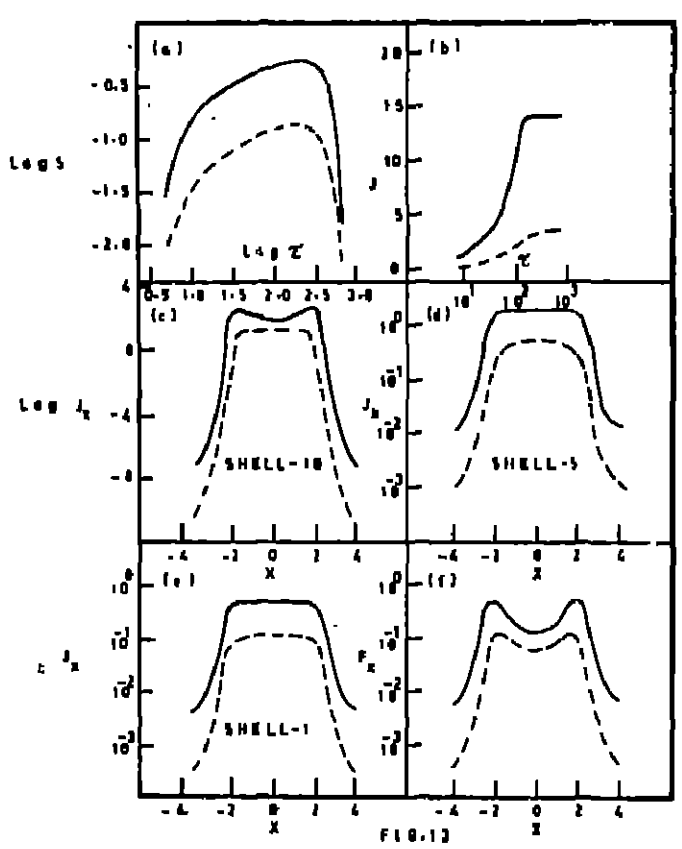

FIG.13

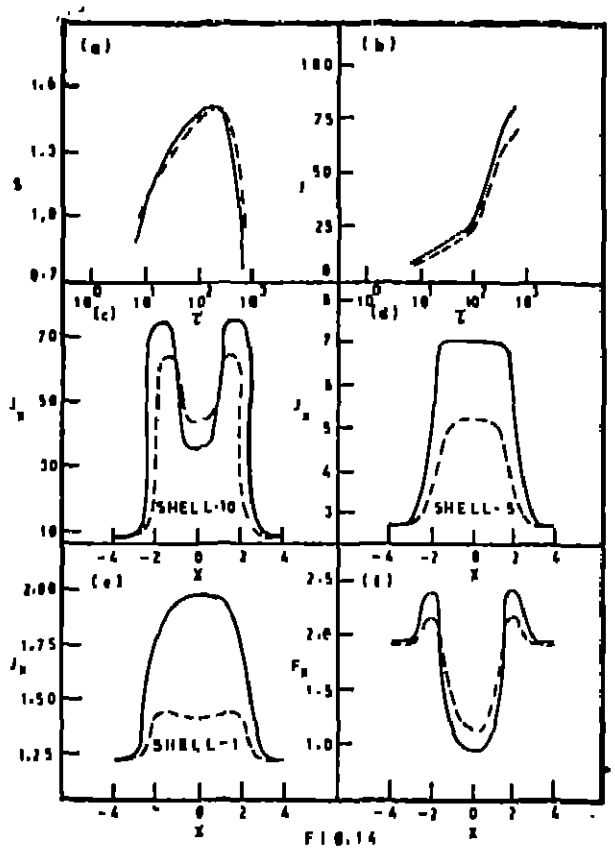

FIG.14

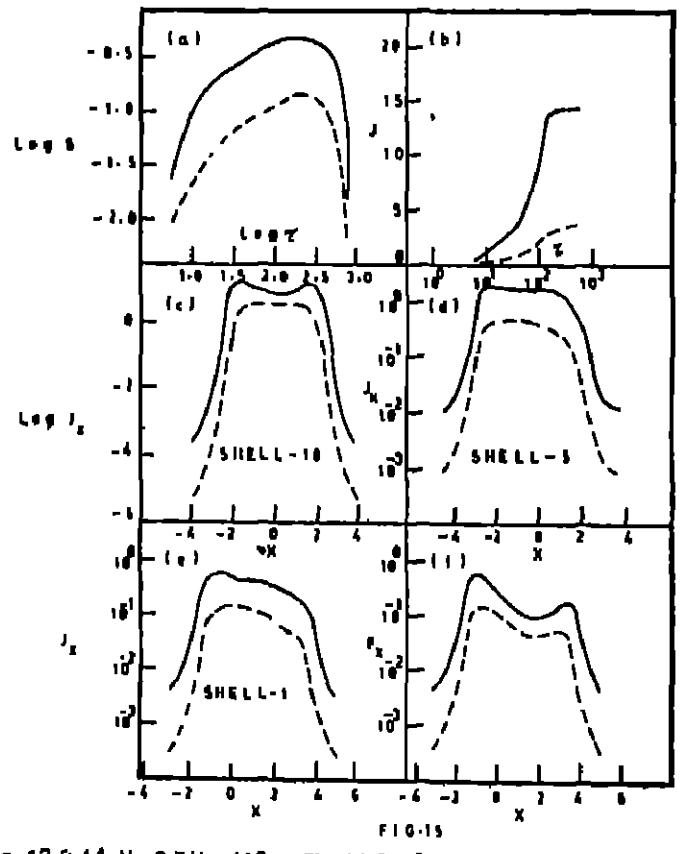

FIG.15

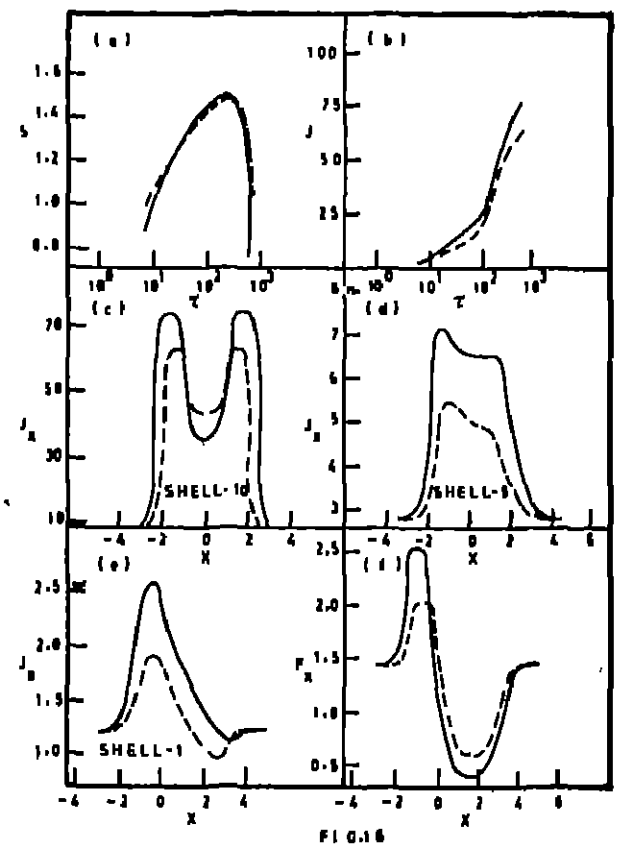

FIG.16

Fig. 13 & 14 V=0 B/A=100. Fig. 15 & 16 V=1 B/A=100. Fig. 13 & 15 $\alpha = 10^{-3}$ $\beta = 0$. Fig. 14 & 16 $\alpha = \beta$ 10^{-3}. CRD, ——— R_{II} - is common for all figures.

and the total mean intensity is given by

$$J_n = \sum_{l=1}^{I} J(x_l, n) A_l \tag{16}$$

We have assumed that the velocity is increasing radially and is given by the relation

$$V_n = V_N + (N - n + \tfrac{1}{2}) \Delta V \tag{17}$$

where V_N is the velocity at the bottom of the atmosphere, V_n is the velocity in current shell number n. The quantity 1/2 is introduced to estimate the velocity in the centre of the shell. And

$$\Delta V = (V_1 - V_N)/N \tag{18}$$

All velocities are measured in units of mean thermal velocity of the gas.

We have presented the results in Figures (1) to (18). In each Figure, we have plotted, the total source functions, and total mean intensity J, versus the optical depth τ, a gradual progression of frequency dependant mean intensities Jx in the line corresponding to shell numbers 10,5 and 1 and the emergent monochromatic flux profiles Fx versus X. Figures (1-2) describe the results for static plane parallel stratification B/A = 1 for the two cases : $\epsilon = 10^{-3}$, $\beta = 0$ and (2) $\epsilon = \beta = 10^{-3}$ respectively. The results in case (1) show central absorption with slight emission in the wings where as the results in case (2) *are totally different* in that the mean intensities at shell 10 show completely absorption feature and those at shell 5 show completely emission and those at shell 1 show absorption feature. The emergent flux profiles in Figure (1) show emission with central absorption and those in Figure (2) form a total absorption line with less than 1% of emission in the wings.

In Figures (3) and (4), we have presented the results for cases (1) and (2) respectively with V = 1 *mean* thermal velocity of the gas in plane parallel medium. Similarly the results in Figures (5) and (6) correspond to cases (1) and (2) for V = 2. When motion is introduced into the gas, we notice that the mean intensity profiles and the emergent flux profiles show asymmetry in their shapes. However, the mean intensity profiles at shell number 10 do not show any asymmetry because the gas at this point is stationary. One also observes the red emission and blue absorption with the centres of the lines shifting towards blue side. The profiles calculated with CRD show larger emission in the case of emission wings or deeper absorption in the case of absorption lines compared to those formed by the PRD function of R_{II}.

In Figures (7) and (8), the results for cases (1) and (2) respectively are presented for B/A = 10 in a stationary medium. The profiles of Figure (1) are quite similar to those of Figure (7) except that there is no central absorption in the mean intensity profiles where as those in Figure (2) are quite different from those given in Figure (8). The mean intensity profile in PP for V = 0 at shell number 1 is completely in absorption (in Fig 2) where as the profiles for B/A = 10 and V = 0 (in Fig 8) at the same radial point are in complete emission while the emergent flux profile is in absorption with 20% of emission in the wings. This is clearly the effect of curvature scattering. Figures (9) and (10) present profiles for V = 1 for the two cases with B/A = 10. The P cygni type profiles are quite prominent in case (2). Figures (11) and (12) give profiles for V = 2. They show similar characteristics shown by those in Figures (9) and (10). Figures (13) to (18) again represent the results for a geometrical extension of B/A = 100 and V = 0, 1 and 2 for the two cases. The effects seen in Figures (7) to (12) are enhanced in these because of more curvature scattering.

Conclusions

We have compared the profiles calculated with CRD and PRD function of R_{II} in a spherically symmetric expanding medium. Those profiles formed in CRD show more emission and deeper absorption wherever these occur compared to those formed by PRD function. Profiles formed in spherically symmetric medium show larger wing emission due to curvature scattering. The extended and expanding medium with emission in the continuum exhibit P cygni type profiles.

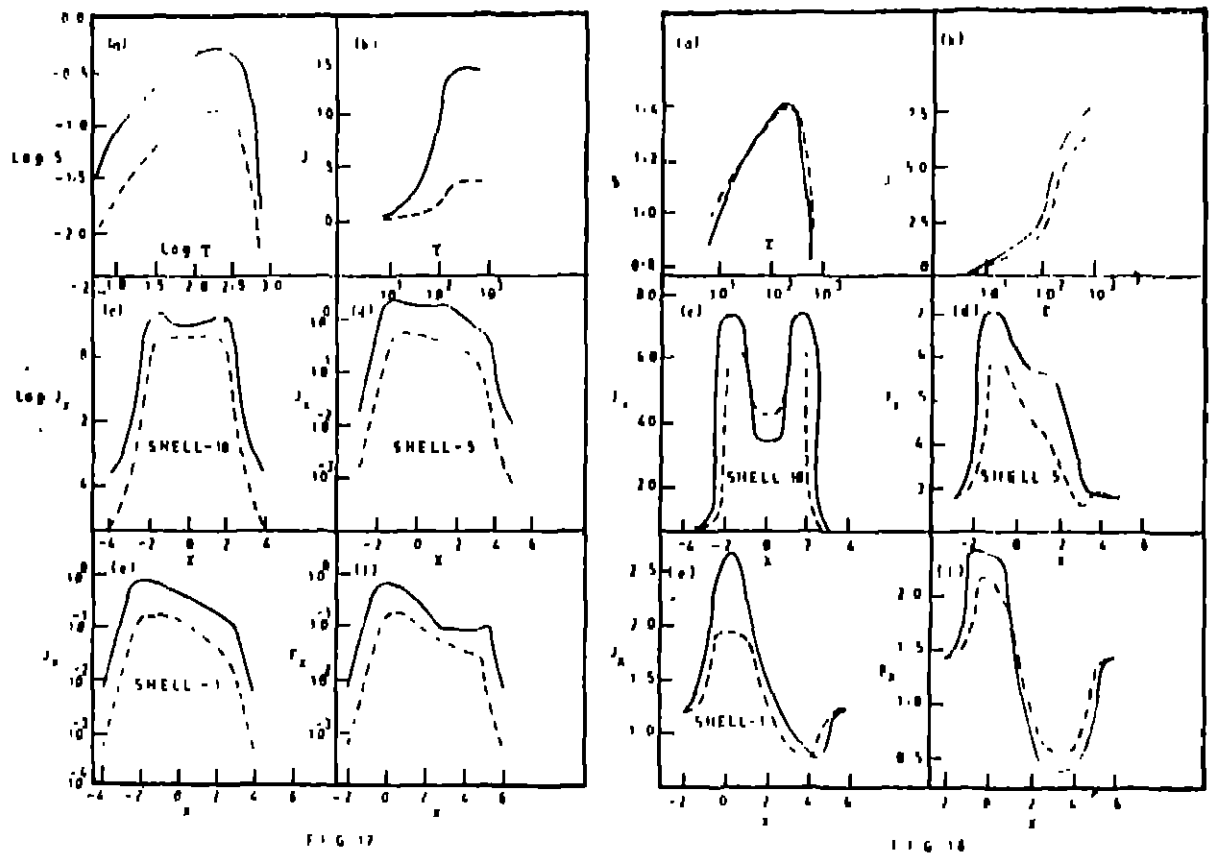

FIG 17 FIG 18

Fig. 17 & 18 V=2 B/A=100 Fig. 17 $\epsilon = \beta = 10^{-3}$. Fig. 18 $\epsilon = 10^{-3}$ $\beta = 0$. _____CRD, – – – RII - le common for four figures

M S received on 25th November 1979

References

Hummer, D. G., 1962, *Mon. Not. R. astr. Soc.* 125, 21.
Hummer, D. G., 1969, *Mon. Not. R. astr. Soc.* 145 95
Jefferies, J. White, D., 1960 *Astrophys. J.* 132, 762
Mihalas, D., 1978, Stellar Atmospheres, 2nd ed, Freeman, San Francisco
Peraiah, A., 1978a, *Astrophys. Space. Sci.* 58, 189
Peraiah, A., 1978b, *Kodaikanal Obs. Bull. Ser. A.* 2, 116.
Peraiah, A., 1979, *Astrophys. Space. Sci.* 63, 267.
Peraiah, A., Grant, I.P., 1973, *J. Inst. Maths. Appl.* 12, 75.
Peraiah, A., Wehrse, R., 1978, *Astron. Astrophys.* 70, 213.
Shine, R. A., Milkey, R. W., Mihalas, D., 1975, *Astrophys. J.* 199, 724.
Vardavas, I. M. 1976, *J.Q.S.R.T.* 16, 901.
Wehrse, R., Peraiah, A., 1979 *Astron. Astrophys.* 71, 289.